

Original Research

Acute Changes in the Resting Brain Networks in Concussion Patients: Small-World Topology Perspective

Hong-mei Kuang¹, Yan Chen¹, Ji-lan Huang¹, Jian Li¹, Ning Zhang¹, Hong-hui Ai^{2,*}, Guo-jin Xia^{1,*}¹Department of Radiology, The First Affiliated Hospital of Nanchang University, 330000 Nanchang, Jiangxi, China²Department of Otolaryngology Head and Neck Surgery, The First Affiliated Hospital of Nanchang University, 330000 Nanchang, Jiangxi, China*Correspondence: aihh@ncu.edu.cn (Hong-hui Ai); ndyfy02344@ncu.edu.cn (Guo-jin Xia)

Academic Editor: Gernot Riedel

Submitted: 6 March 2023 Revised: 8 May 2023 Accepted: 22 May 2023 Published: 16 January 2024

Abstract

Background: The acute changes that occur in the small-world topology of the brain in concussion patients remain unclear. Here, we investigated acute changes in the small-world organization of brain networks in concussion patients and their influence on persistent post-concussion symptoms. **Methods:** Eighteen concussion patients and eighteen age-matched controls were enrolled in this study. All participants underwent computed tomography, magnetic resonance imaging (MRI), susceptibility weighted imaging, and blood oxygen level-dependent functional MRI. A complex network analysis method based on graph theory was used to calculate the parameters of small-world networks under different degrees of network sparsity. All subjects were evaluated using the Glasgow Coma Scale and Rivermead Postconcussion Symptom Questionnaire. **Results:** Compared with the controls, the normalized cluster coefficient (γ) of whole brain networks in patients and the “small-world” index (σ) was slightly enhanced, whereas the standardized minimum path (λ) was slightly shorter. Whole brain effect (Eglobal) and local effect (Elocal) changes were not pronounced. Under the condition of minimum network sparsity ($D_{min} = 0.13$), the numbers of nodes in the “right intraorbital superior frontal gyrus” (Anatomical Automatic Labeling, AAL26), right globus pallidus (AAL76), and bilateral temporal transverse gyrus (AAL79,80) in brain concussion patients were significantly lower. The numbers of nodes in the left subcapital lobe (AAL61) and left occipital gyrus (AAL51) were significantly higher, and the normalized cluster coefficients of the right intraorbital supraphallus (AAL26) and left posterior cingulate gyrus (AAL35) were significantly increased. The normalized clustering coefficients of the right triangular subfrontal gyrus (AAL55) (based on the normalized clustering coefficients of nodes in AAL14) and left sub-parietal lobes (AAL61) were significantly reduced. The mean local effects of nodes in the right intraorbital upper frontal gyrus (AAL26), left posterior cingulate gyrus (AAL35), and bilateral auxiliary motor cortex (AAL19, 20) were enhanced, whereas the mean local effects of the bilateral triangular inferior frontal gyrus (AAL13,14) and left insular cap (AAL11) were reduced ($p < 0.05$). **Conclusions:** The overall trend of network topology abnormalities in patients was random, and generalized and local functional abnormalities were seen. Changes in the function and affective circuitry of the resting default network were particularly pronounced in these patients, which we speculate may be one of the main drivers of the cognitive dysfunction and mood changes seen in concussion patients.

Keywords: brain networks; small-world topology; concussion; changes

1. Introduction

Concussion (sometimes called brain concussion, BC) is an important subtype of mild traumatic brain injury (mTBI), a condition in which the brain cortex is suppressed due to transient dysfunction of the brainstem reticular system after traumatic brain injury (TBI). Its main characteristics are short-term impaired consciousness; short-term retrograde amnesia after waking up but no organic damage, which is clinically easy to ignore due to its mild, short-duration symptoms; and a self-limiting nature [1]. However, about 10–15% of patients have symptoms for >10 days, which may even last for months or an entire lifetime, potentially seriously affecting their work and daily life. This condition is referred to as persistent post-concussion symptoms (PCS), and is mainly characterized by cognitive, emotional, physical, and sleep disorders [2,3]. Pre-

viously, concussion patients commonly underwent routine computed tomography (CT) scans to exclude damage to the brain structure after trauma. However, given that susceptibility weighted imaging (SWI) has greatly improved the detection rate of microhemorrhages, it can help determine the reasons for the persistence of symptoms in BC patients. However, questions remain regarding the persistence of PCS in BC patients with negative SWI findings; thus, further investigation of the connections among functional networks is needed.

The brain is an extensive, interactive, complex network with topological properties [4]. He *et al.* [5] successfully constructed the first human brain structural network in 2007 and found that the network has a “small-world” characteristic. Several subsequent studies have shown that brain networks have small-world properties and exhibit varying



degrees of damage among different diseases [6–9]. Zhou *et al.* [10] and Johnson *et al.* [11] reported that the default mode network (DMN) is the major functional network disrupted after concussion in the absence of structural deficits. Some researchers in the Salience Network found decreased functional connectivity after concussion [12,13]. To date, there are few literatures reports on acute changes in the small-world properties of the brain in concussion patients.

In this study, a complex network analysis method was used to observe acute changes in the brain network topology of BC patients in the resting state, and the influence of these changes on PCS and possible mechanisms. The results of this study provide some insights into the central pathophysiology of BC patients with negative traditional imaging findings.

2. Materials and Methods

2.1 Participants and Ethics Statement

All of the participants or guardians provided informed written consent prior to study enrollment. The study protocol was approved by the Human Research Ethics Committee and Institutional Review Board of the First Affiliated Hospital of Nanchang University. The project was based on the Clinical Research Center For Medical Imaging In Jiangxi Province (No.20223BCG74001). All study procedures were carried out in accordance with approved guidelines and the principles of the Declaration of Helsinki. All BC patients were retrospectively selected from a TBI database ($n = 162$) comprising multimodal magnetic resonance imaging (MRI) results. The inclusion criteria for BC patients were as follows: met the diagnostic criteria for mTBI of the American Congress of Rehabilitation Medicine; presented within 24 h of injury with a Glasgow Coma Scale (GCS) score of 13–15; negative CT, MRI, and SWI findings for brain tissue; age <60 years (to avoid possible effects of physiological atrophy), and underwent a voluntarily MRI examination within 7 days after their injury, along with clinical tests on the day of scanning and 10 days after injury. The exclusion criteria were as follows: previous history of brain trauma, mental illness or drug addiction; and contraindications to MRI examination (e.g., metal dentures, pacemakers). All matched healthy controls (HCs) were recruited from the local community and had no history of neurological or psychiatric disorders.

2.2 Data Acquisition and Clinical Assessment

MRI scanning was performed at our hospital using a 3.0-Tesla MRI system (Trio, Siemens Healthcare, Erlangen, Germany). High-resolution T1-weighted anatomical images were acquired using a sagittal magnetization-prepared rapid acquisition gradient echo sequence for optimal gray-white matter contrast, with the following parameter settings: repetition time (TR) = 1900 ms, echo time (TE) = 2.26 ms, flip angle = 15°, the field of view (FOV) = 215

mm × 230 mm, and slice number = 176. Functional MRI (fMRI) data were acquired using an interleaved axial echo-planar imaging sequence (TR = 2000 ms, TE = 30 ms, FOV = 200 mm × 200 mm, flip angle = 90°, slice number = 30). During the fMRI scan, the subjects were asked to keep their eyes closed, remain as motionless as possible, and avoid thinking systematically. Additional conventional T2-weighted (TR/TE = 4000/113 ms, slice thickness = 5 mm, matrix = 320 × 256), T2-fluid-attenuated inversion recovery (TR/TE/TI (inversion time) = 8000/79/2722 ms, slice thickness = 5 mm, matrix = 320 × 256), SWI (TR/TE = 28/20 ms, flip angle = 15°, slice thickness = 1.2 mm, matrix = 320 × 256), and diffusion weighted imaging (TR/TE = 3100/91 ms, $b = 1000 \text{ s/mm}^2$, matrix = 192 × 192) scans were obtained.

Each patient underwent a detailed clinical interview and physical examination, including the GCS and Rivermead Postconcussion Symptoms Questionnaire (RPQ), on the day of the scan and after the acute phase of trauma. All demographic and clinical assessment results were compared between the two groups using SPSS 20.0 software (IBM Inc., Chicago, IL, USA).

2.3 Data Analysis

Blood oxygen level-dependent fMRI data were obtained using Onis 2.5 (<http://www.onis-viewer.com>) software. The brain was divided into 90 regions according to the Anatomical Automated Labeling templates provided by the brain network analysis and visualization software packages Gretna and BrainNet Viewer (<https://www.nitrc.org/projects/bnv/>). The time series for each voxel was calculated in each region and averaged. Pearson's correlation coefficient between two regions was calculated to construct a symmetrical correlation matrix, which was then subjected to Fisher Z transformation for conversion to a binary connectivity matrix. After obtaining the binary matrix, a binarized function of the brain was constructed to connect the brain network, and the topological properties of the network under different degrees of sparsity (i.e., network density) were calculated including the clustering coefficient, shortest path length, and σ , among other indicators.

The clustering coefficient (C) reflects the local separation of the network and corresponds to the mean clustering coefficient for all nodes (i) therein. The number of edges (e_i) near a node adjacent to an actual connection was divided by the maximum number of sides (k) that could be connected ($k_i [k_i - 1]$). Thus, the cluster coefficient of the node C_i is given by $C_i = 2e_i / k_i [k_i - 1]$.

The shortest path length (L) reflects the whole brain integration effect and represents the best path in the network from one node (i) to another node (j). The shortest path length of each node was averaged to obtain L.

Notably, for the abovementioned parameters, the actual brain network topology attributes of each subject were normalized (divided by the corresponding attributes of 1000

Functional Connectivity Matrix

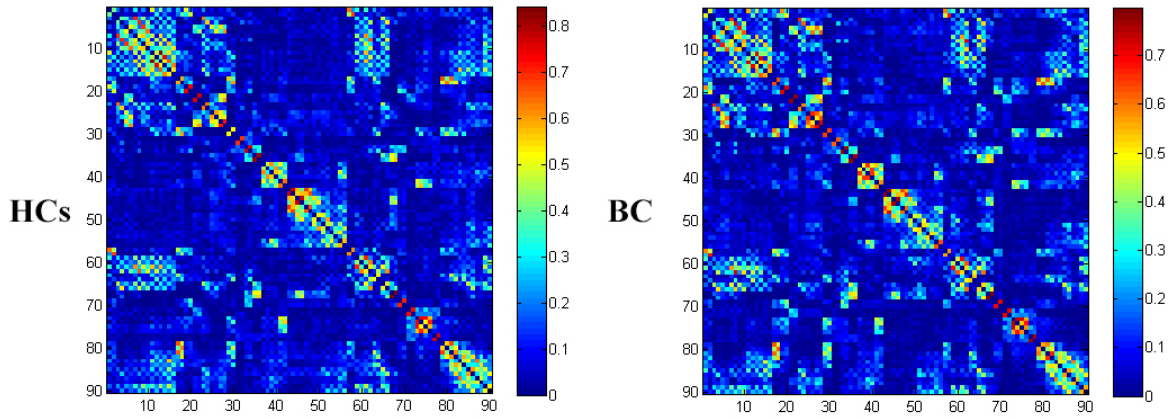


Fig. 1. Functional correlation matrix in the healthy control (HC) group (left) and brain concussion (BC) group (right) under the minimum network sparsity ($D_{min} = 0.13$).

random networks) to obtain the normalized cluster coefficients ($\gamma = C/C_{rand}$) and standardized path length ($\lambda = L/L_{rand}$).

The small world index ($\sigma = \gamma/\lambda$) reflects more efficient network characteristics (i.e., the highest cluster coefficient and shortest path length). When the characteristics of a network show that $\gamma_i/\gamma_{rand} > 1$, γ_i tends to γ_p , and λ_i/λ_{rand} is close to 1, $\sigma_i > 1$, indicating that the network has small-world characteristics, where “P” represents a regular network and “rand” represents a random network.

Other indicators included whole brain efficiency, local efficiency, and node betweenness. Differences in network graph theory metrics were determined by calculating the area under the curve across all sparsities and using analysis of variance and post-hoc analysis with age and sex as covariates and the false discovery rate correction, $q = 0.05$. An independent two-sample t -test was used for the comparisons. $p < 0.05$ was considered statistically significant.

3. Results

3.1 Comparison of General and Clinical Scoring Scales

In this study, 18 patients (9 men and 9 women) with acute-stage BC who met the requirements were selected from the TBI database; they were all right-handed, had an average age of 36.8 ± 12.2 (20–56) years, have an average time since the injury of 3.6 ± 2.3 (0.5–7) days, and an average of 7.2 ± 3.1 (2–15) years of education. Eighteen HCs were matched by sex, age, and educational attainment; there was no statistically significant difference in age or years of education between the two groups ($p > 0.05$). The GCS scores of BC patients and the HCs did not show statistically significant differences. The RPQ score was significantly higher for the patients than HCs ($p = 0.001$), as shown in Table 1.

Table 1. General characteristics and clinical data of the BC and HC groups.

General information	BC	HCS	t	p
Age (y)	36.8 ± 12.2	36.4 ± 11.1	0.086	0.932
Sex (m/f)	9/9	9/9	-	-
Education (years)	7.2 ± 3.1	7.1 ± 2.8	0.056	0.956
Time since injury (days)	3.6 ± 2.3	-	-	-
GCS score	14.9 ± 0.3	15 ± 0	-1.458	0.163
RPQ score	28.5 ± 8.9	0	13.617	0.000*

BC, brain concussion; HC, healthy control; GCS, Glasgow Coma Scale; RPQ, Rivermead Postconcussion Symptom Questionnaire.

Age, education, illness duration, GCS, and RPQ data are shown as the mean \pm standard deviation. *statistically significant difference.

3.2 Changes in Small-World Topology

Using different correlation coefficients as thresholds to define network sparsity, a 90×90 binary function connection matrix was constructed, as shown in Fig. 1.

3.2.1 Measurement and Comparison of the Overall Properties of Brain Functional Networks

After measuring the overall properties of brain functional networks under different network sparsity conditions, cluster coefficients and shortest path lengths were standardized to obtain standardized cluster coefficients (γ), standardized shortest path lengths (λ), and the σ (Fig. 2A–C, respectively). The minimum network sparsity (D_{min}) of 0.13 was used to ensure the full connection of brain functional network nodes. The maximum sparseness (D_{max}) of the small world characteristic ($\sigma > 1$) of the brain functional networks of the BC and HC groups was 0.48. Compared with the HC group, the γ value of the BC group was

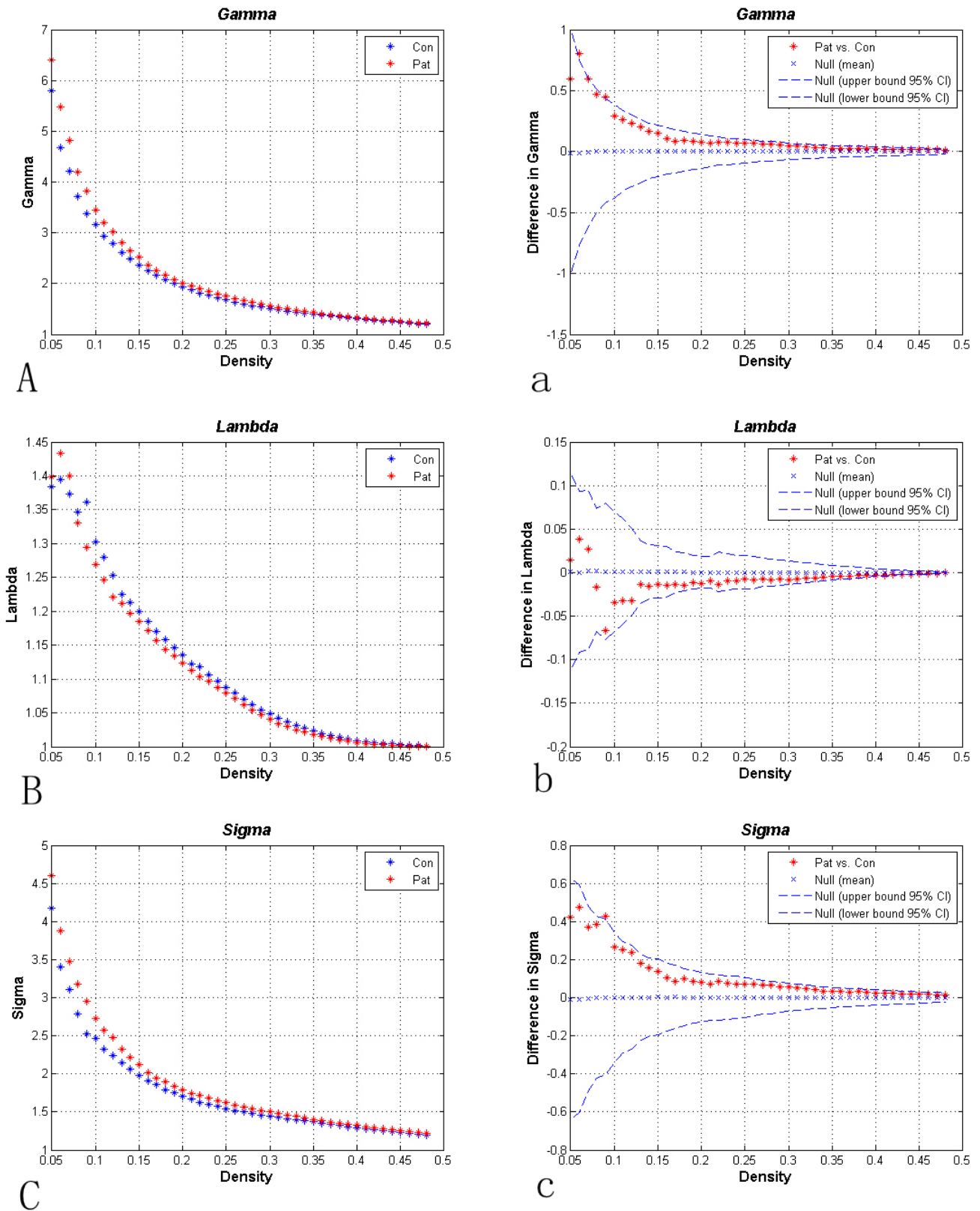


Fig. 2. Overall properties of brain networks under different sparsity conditions. Plates (A–C) show the standardized cluster coefficients (A), standardized shortest path length (B), and “small-world” index (σ) (C) of the brain concussion (BC) and healthy control groups. Both groups had small-world characteristics ($\sigma > 1$). Within the network sparsity range (0.13–0.48), the brain network standardized cluster coefficient (a) was slightly increased in the BC group, the standardized minimum path length (b) was slightly reduced, and σ (c) was slightly higher; however, the group differences were not statistically significant ($p > 0.05$). CI, Confidence Interval.

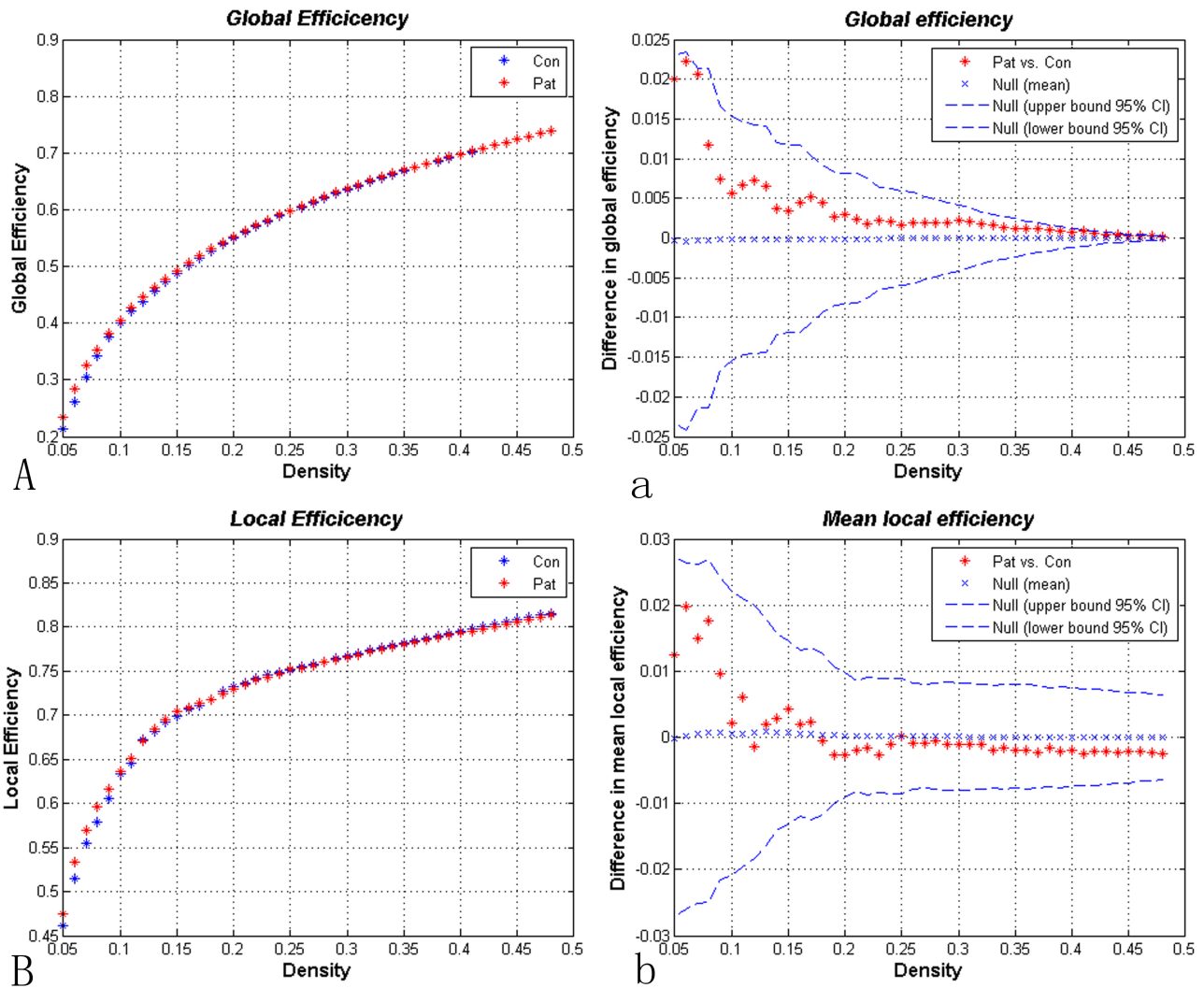


Fig. 3. Small-world network efficiency results obtained within the network sparsity range. Compared with the healthy control group, whole brain (A and a) and local measurements (B and b) were not significantly different in the brain concussion group.

slightly higher (Fig. 2a). The λ value was slightly lower (Fig. 2b), but within the range of network sparsity (0.13–0.48); the difference was not statistically significant ($p > 0.05$). Overall, these changes resulted in a slight increase in the σ values of the functional networks in the BC group (Fig. 2c; $p > 0.05$).

3.2.2 Measurement and Comparison of Brain Functional Network Efficiency

In the small-world network density range of the BC and HC groups, differences in brain function network effect parameters, including the whole brain effect (Eglobal) and local effect (Elocal), were not statistically significant under the same network sparsity conditions (Fig. 3).

3.2.3 Comparison of Local Parameters of Brain Functional Networks

Under the condition of $D_{min} = 0.13$, node betweenness in the right intraorbital superior frontal gyrus (ORB-

supmed.R, AAL26, Anatomical Automatic Labeling), right globus pallidus (PAL, AAL76), and Heschl's gyrus (HG), also known as transverse temporal gyrus (AAL77 and AAL78) in the BC patient group were significantly lower ($p < 0.05$), whereas node betweenness between the left inferior parietal lobe (IPL.L, AAL61) and median occipital gyrus (MOG, AAL51) was significantly higher ($p < 0.05$; Fig. 4).

The normalized cluster coefficients of the ORB-supmed.R (AAL26) and left posterior cingulate gyrus (PCG, AAL35) in the BC group were significantly higher ($p < 0.05$). The normalized cluster coefficients of the inferior frontal gyrus pars triangularis (IFGtriang, AAL14) and IPL (AAL61) were significantly reduced ($p < 0.05$). Normalized clustering coefficients for other nodes within the functional brain network showed a slight increase or decrease ($p > 0.05$; Fig. 5A,a). Enhanced local nodal effects ($p < 0.05$) were observed for the right ORBsupmed (AAL26), left PCG (AAL35), and bilateral supplementary motor area

Node Betweenness

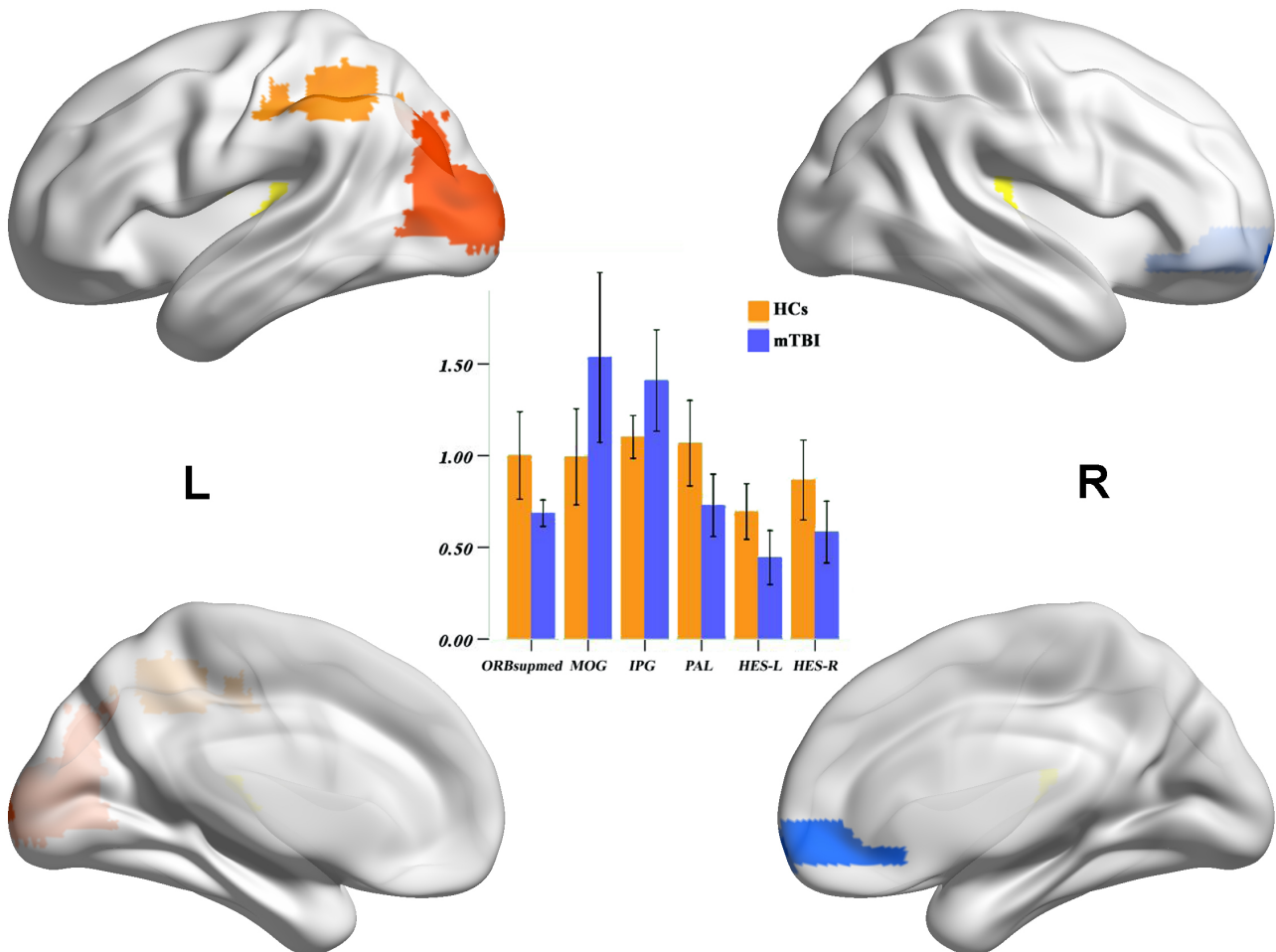


Fig. 4. Comparison of node betweenness under the minimum network sparsity condition ($D_{min} = 0.13$). Compared with the healthy control (HC) group, node betweenness in the right intraorbital superior frontal gyrus (ORBsupmed.R, right globus pallidus), and bilateral temporal traverse (Heschl's gyrus) in the BC group were significantly lower, whereas node betweenness in the left inferior parietal lobule (IPL.L) and left median occipital gyrus (MOG) were significantly higher ($p < 0.05$). mTBI, mild traumatic brain injury; PAL, pallidus.

(SMA, AAL19, and AAL20) in the BC group. A reduction in local nodal effects was observed between the bilateral triangular inferior frontal gyrus (IFGtriang, AAL13 and AAL14) and the left insular cap inferior frontal gyrus (IFGopere, AAL11) ($p < 0.05$). The local effects of other nodes in the functional network showed a slight increase or decrease ($p > 0.05$; Fig. 5B,b).

4. Discussion

The human brain is a complex, internally connected system, with a highly diverse set of important topological attributes such as small-world attributes, low efficiency, and high connectivity of hub nodes [14,15]. The small-world network model, also known as the Watt–Strogatz model [16], combines the characteristics of shortest path

length and high cluster coefficients and provides a powerful means for interpreting brain network models. The combination of high cluster coefficients and the shortest path length reflects two important attributes for the management of the human brain: functional separation and functional integration.

Our complex network analysis based on graph theory revealed that both the BC patient and normal control groups had efficient small-world attributes in whole-brain functional networks (>1). Many studies have shown that both healthy people and patients with brain damage, for example due to hepatic encephalopathy [17], drug addiction [18], Alzheimer's disease (AD) [19], and multiple sclerosis [20], do not show changes in the overall nature of the small-world brain network, although certain parameters are abnormal. The results of this study are consistent with this premise.

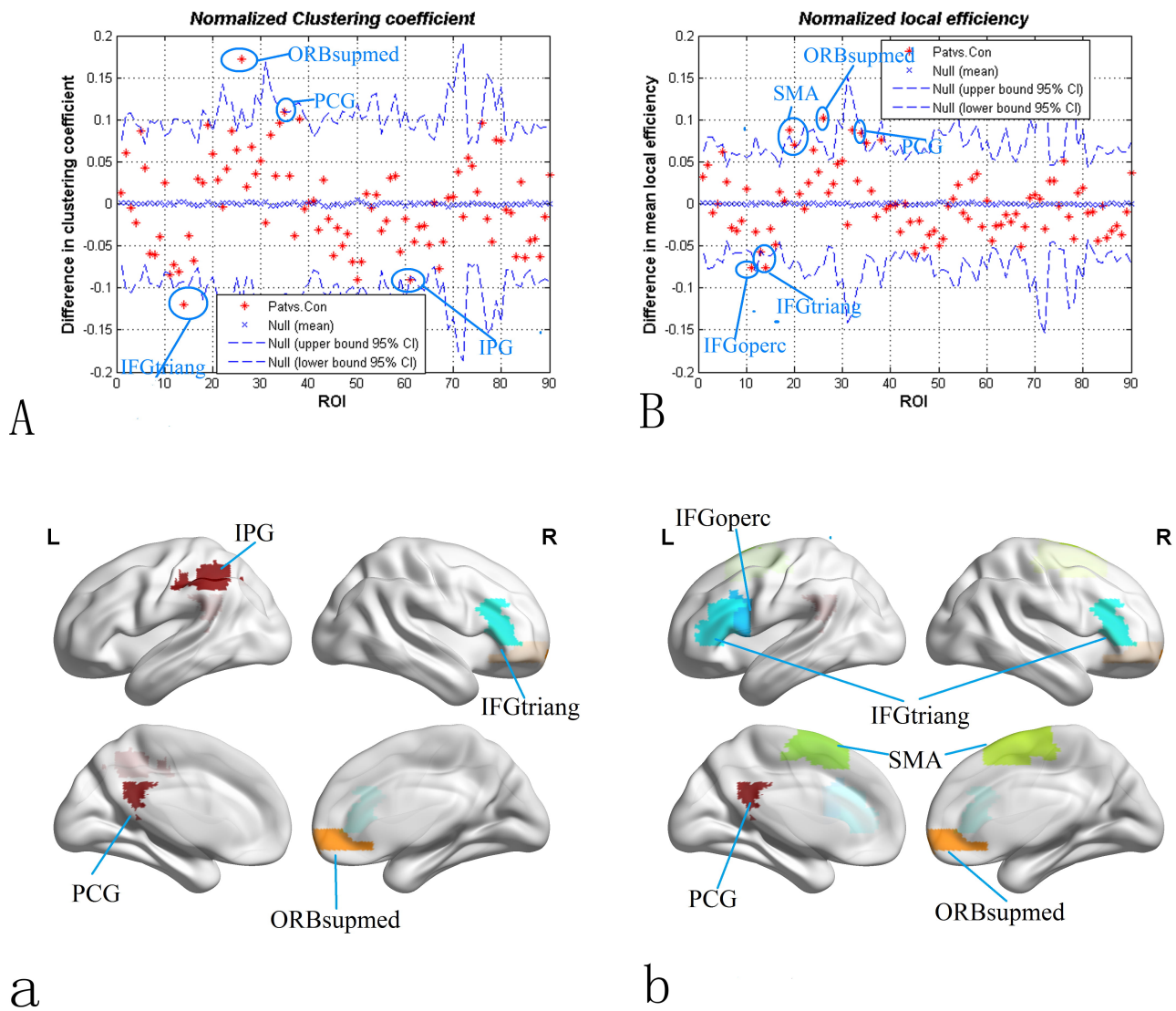


Fig. 5. Under the minimum network sparsity condition ($D_{min} = 0.13$), clustering coefficients (plates A and a), and local node effects (plates B and b) were compared between the groups for each brain region. Compared with the healthy control group, the standardized cluster coefficients of the right intraorbital superior frontal gyrus (ORBsupmed) and left posterior cingulate gyrus (PCG) were significantly higher in the patient group, whereas the normalized cluster coefficients of the right triangular inferior frontal gyrus (IFGtriang) and left inferior parietal lobules (IPLs) were significantly lower ($p < 0.05$) (plates A and a). Local effects of nodes in the right intraorbital upper frontal gyrus (ORBsupmed), left PCG, and bilateral auxiliary motor cortex (supplementary motor area [SMA]) were enhanced in the patient group, but were reduced ($p < 0.05$) (blue circles) between the bilateral triangular inferior frontal gyrus (IFGtriang and left insular cap inferior frontal gyrus [IFGoperc]) (plates B and b). ROI, region of interest; IPG, inferior parietal gyrus.

We found that although the two groups showed common small-world topological properties, there were still several important differences. Specifically, the standardized clustering coefficient and shortest path length of the brain network of BC patients were slightly elevated and shorter, respectively, resulting in a slight increase in the σ of the brain network. Most of the intergroup network properties were in the range of network sparsity (0.13–0.48), indicating that there were no isolated and/or network nodes in the fully connected network. In this range, the above three brain net-

work indicators were not statistically significant in patients with BC. The result was consistent with the study of Virji-Babul *et al.* [21]. This suggests a tendency for the network indicators of functional networks to increase in BC patients, indicating that the balance between functional integration and separation in their small-world networks is disturbed (i.e., closer to random). This randomization is also seen in AD [19] and schizophrenia [22]. Random networks exhibit less modular information processing and lower fault tolerance than small-world networks; thus, the small-world net-

works of BC patients deviate from the optimal brain topological network structure. Our small-world network results were consistent with other TBI studies [23,24]; the slight differences may be explained by differences in patient inclusion criteria.

We observed no significant differences in the whole brain or meant local efficiency between the BC and HC groups. However, there were significant differences in the local efficiency of some brain regions, suggesting compensatory changes in the brain network of concussion patients. This was consistent with Yan's study [25] but was inconsistent with Churchill's study [26]; the slight differences may be explained by differences in patient inclusion criteria and too few samples. Regarding the right medial orbitofrontal cortex, left posterior cingulate gyrus, and left sub-parietal lobules (i.e., the core area of the DMN), an increase in the local efficiency was seen in the former two and a reduction was seen in the latter, suggesting functional separation of the DMN. Functional separation of the DMN was consistent with some smaller research results [10,27]. A sleep deprivation study by Gujar *et al.* [28] revealed the bidirectional separation of DMN function; combined with the results of this study, we speculate that the function of some brain areas of the DMN after BC injury may be impaired, while other brain regions provide complementary functionality. Alternatively, different brain regions within the DMN may control different subfunctions, where compensation by one side due to functional impairment of the other side may result in the separation of DMN function [10]. The specific mechanism requires further study.

This study also found that compared with the HC group, the nature of brain network nodes in BC patients was consistently altered, which was mainly reflected in abnormal changes in emotional circuits. The cluster coefficient and average local effect of the upper frontal node on the right orbit were increased, while the median number of nodes was reduced, in the BC group. The former two findings reflect the enhancement of node betweenness, which indicates that the influence of nodes in the functional loop was weakened. The intraorbital prefrontal gyrus is associated with the prefrontal lobe system and abnormal emotional processing. Abnormal changes in the frontal gyrus contribute to emotional numbness, mental alertness, and psychological avoidance in patients with post-traumatic stress disorder [29]. The superior frontal triangle and the superior frontal insular gyrus are part of the frontal gyrus; a change in the nature of their nodes may contribute to the abnormal brain emotional circuits seen in BC patients. The PAL is part of the limbic system and is involved in emotional processing. The reduction in the number of nodes in the left PAL seen in this study may play a role in the negative mood of BC patients. Functional separation of the nodes in the core area of the DMN was also seen, as stated above. The number of nodes mediating the hearing-related brain region (bilateral temporal transverse gyrus) is

reduced, whereas the number in the vision-related brain region (left occipital midgyrus) is increased, in BC patients, which may explain their noise sensitivity. The left occipital midgyrus is associated with the visual cortex, and plays a role in mild cognitive impairment and early manifestations of AD [19]. These abnormalities may explain some of the symptoms of BC, but their clinical relevance has yet to be explored.

Limitations

The clinical scoring scale of patients in this study had few categories and lacked a follow-up study. The range of education level and age in this patient group was large and the number of cases was relatively small, which was not enough to group patients with different levels of education and age. This study did not study the correlation between topology attribute parameters and clinical scales. We expect this to be further studied in the future.

5. Conclusions

In patients with concussion, random abnormalities may be seen in the overall and local properties of the resting brain functional network. Functional abnormalities in the default network and changes in the emotional circuit in the resting state are particularly significant. We speculate that these abnormalities may lead to cognitive dysfunction and emotional changes in BC patients.

Abbreviations

BC, brain concussion; HC, healthy control; GCS, Glasgow Coma Scale; RPQ, Rivermead Postconcussion Symptom Questionnaire; MRI, magnetic resonance imaging; mTBI, mild traumatic brain injury; PCS, post-concussion symptoms; CT, computed tomography; SWI, susceptibility weighted imaging; DMN, default mode network.

Availability of Data and Materials

The datasets used and/or analysed during the current study are available from the corresponding author on reasonable request.

Author Contributions

HHA and GJX designed the research study. HMK and YC performed the research. GJX provided help and advice on research. JLH and JL analyzed the data. NZ contributed analytic tools and finalized the manuscript, HMK, NZ and JLH participated in the writing of the manuscript. All authors contributed to editorial changes in the manuscript. All authors read and approved the final manuscript. All authors have participated sufficiently in the work and agreed to be accountable for all aspects of the work.

Ethics Approval and Consent to Participate

All of the participants or guardians provided informed written consent prior to study enrollment. The study protocol was approved by the Human Research Ethics Committee and Institutional Review Board of the First Affiliated Hospital of Nanchang University (No: (2022)CDYFYLYK(09-043)). All study procedures were carried out in accordance with approved guidelines and the principles of the Declaration of Helsinki.

Acknowledgment

We would like to thank two professional editors for helping polishing the English language.

Funding

This research received no external funding.

Conflict of Interest

The authors declare no conflict of interest.

References

- [1] Yeates KO. Mild traumatic brain injury and postconcussive symptoms in children and adolescents. *Journal of the International Neuropsychological Society: JINS*. 2010; 16: 953–960.
- [2] Webbe FM, Barth JT. Short-term and long-term outcome of athletic closed head injuries. *Clinics in Sports Medicine*. 2003; 22: 577–592.
- [3] Bigler ED. Neuropsychology and clinical neuroscience of persistent post-concussive syndrome. *Journal of the International Neuropsychological Society: JINS*. 2008; 14: 1–22.
- [4] Nemzer LR, Cravens GD, Worth RM, Motta F, Placzek A, Castro V, *et al.* Critical and Ictal Phases in Simulated EEG Signals on a Small-World Network. *Frontiers in Computational Neuroscience*. 2021; 14: 583350.
- [5] He Y, Chen ZJ, Evans AC. Small-world anatomical networks in the human brain revealed by cortical thickness from MRI. *Cerebral Cortex (New York, N.Y.: 1991)*. 2007; 17: 2407–2419.
- [6] Stam CJ, Jones BF, Nolte G, Breakspear M, Scheltens P. Small-world networks and functional connectivity in Alzheimer's disease. *Cerebral Cortex (New York, N.Y.: 1991)*. 2007; 17: 92–99.
- [7] Liu Y, Liang M, Zhou Y, He Y, Hao Y, Song M, *et al.* Disrupted small-world networks in schizophrenia. *Brain: a Journal of Neurology*. 2008; 131: 945–961.
- [8] He Y, Chen Z, Evans A. Structural insights into aberrant topological patterns of large-scale cortical networks in Alzheimer's disease. *The Journal of Neuroscience: the Official Journal of the Society for Neuroscience*. 2008; 28: 4756–4766.
- [9] He Y, Dagher A, Chen Z, Charil A, Zijdenbos A, Worsley K, *et al.* Impaired small-world efficiency in structural cortical networks in multiple sclerosis associated with white matter lesion load. *Brain: a Journal of Neurology*. 2009; 132: 3366–3379.
- [10] Zhou Y, Milham MP, Lui YW, Miles L, Reaume J, Sodickson DK, *et al.* Default-mode network disruption in mild traumatic brain injury. *Radiology*. 2012; 265: 882–892.
- [11] Johnson B, Zhang K, Gay M, Horovitz S, Hallett M, Sebastianelli W, *et al.* Alteration of brain default network in subacute phase of injury in concussed individuals: resting-state fMRI study. *NeuroImage*. 2012; 59: 511–518.
- [12] Zhan J, Gao L, Zhou F, Kuang H, Zhao J, Wang S, *et al.* Decreased Regional Homogeneity in Patients With Acute Mild Traumatic Brain Injury: A Resting-State fMRI Study. *The Journal of Nervous and Mental Disease*. 2015; 203: 786–791.
- [13] Peters SK, Dunlop K, Downar J. Cortico-Striatal-Thalamic Loop Circuits of the Salience Network: A Central Pathway in Psychiatric Disease and Treatment. *Frontiers in Systems Neuroscience*. 2016; 10: 104.
- [14] Bullmore ET, Bassett DS. Brain graphs: graphical models of the human brain connectome. *Annual Review of Clinical Psychology*. 2011; 7: 113–140.
- [15] Sporns O. The human connectome: a complex network. *Annals of the New York Academy of Sciences*. 2011; 1224: 109–125.
- [16] Watts DJ, Strogatz SH. Collective dynamics of 'small-world' networks. *Nature*. 1998; 393: 440–442.
- [17] Hsu TW, Wu CW, Cheng YF, Chen HL, Lu CH, Cho KH, *et al.* Impaired small-world network efficiency and dynamic functional distribution in patients with cirrhosis. *PLoS ONE*. 2012; 7: e35266.
- [18] Zhang J, Wang J, Wu Q, Kuang W, Huang X, He Y, *et al.* Disrupted brain connectivity networks in drug-naive, first-episode major depressive disorder. *Biological Psychiatry*. 2011; 70: 334–342.
- [19] Stam CJ, de Haan W, Daffertshofer A, Jones BF, Manshanden I, van Cappellen van Walsum AM, *et al.* Graph theoretical analysis of magnetoencephalographic functional connectivity in Alzheimer's disease. *Brain: a Journal of Neurology*. 2009; 132: 213–224.
- [20] Fuchs TA, Ziccardi S, Benedict RHB, Bartnik A, Kuceyeski A, Charvet LE, *et al.* Functional Connectivity and Structural Disruption in the Default-Mode Network Predicts Cognitive Rehabilitation Outcomes in Multiple Sclerosis. *Journal of Neuroimaging: Official Journal of the American Society of Neuroimaging*. 2020; 30: 523–530.
- [21] Virji-Babul N, Hilderman CGE, Makan N, Liu A, Smith-Forrester J, Franks C, *et al.* Changes in functional brain networks following sports-related concussion in adolescents. *Journal of Neurotrauma*. 2014; 31: 1914–1919.
- [22] Lynall ME, Bassett DS, Kerwin R, McKenna PJ, Kitzbichler M, Muller U, *et al.* Functional connectivity and brain networks in schizophrenia. *The Journal of Neuroscience: the Official Journal of the Society for Neuroscience*. 2010; 30: 9477–9487.
- [23] Imms P, Clemente A, Cook M, D'Souza W, Wilson PH, Jones DK, *et al.* The structural connectome in traumatic brain injury: A meta-analysis of graph metrics. *Neuroscience and Biobehavioral Reviews*. 2019; 99: 128–137.
- [24] Rowland JA, Stapleton-Kotloski JR, Dobbins DL, Rogers E, Godwin DW, Taber KH. Increased Small-World Network Topology Following Deployment-Acquired Traumatic Brain Injury Associated with the Development of Post-Traumatic Stress Disorder. *Brain Connectivity*. 2018; 8: 205–211.
- [25] Yan Y, Song J, Xu G, Yao S, Cao C, Li C, *et al.* Correlation between standardized assessment of concussion scores and small-world brain network in mild traumatic brain injury. *Journal of Clinical Neuroscience: Official Journal of the Neurosurgical Society of Australasia*. 2017; 44: 114–121.
- [26] Churchill NW, Hutchison MG, Graham SJ, Schweizer TA. Long-term changes in the small-world organization of brain networks after concussion. *Scientific Reports*. 2021; 11: 6862.
- [27] Sours C, Zhuo J, Janowich J, Aarabi B, Shanmuganathan K, Gulapalli RP. Default mode network interference in mild traumatic brain injury - a pilot resting state study. *Brain Research*. 2013; 1537: 201–215.
- [28] Gujar N, Yoo SS, Hu P, Walker MP. The unrested resting brain: sleep deprivation alters activity within the default-mode network. *Journal of Cognitive Neuroscience*. 2010; 22: 1637–1648.
- [29] Lee GP, Meador KJ, Loring DW, Allison JD, Brown WS, Paul LK, *et al.* Neural substrates of emotion as revealed by functional magnetic resonance imaging. *Cognitive and Behavioral Neurology: Official Journal of the Society for Behavioral and Cognitive Neurology*. 2004; 17: 9–17.